

# cPKC $\gamma$ -mediated down-regulation of UCHL1 alleviates ischaemic neuronal injuries by decreasing autophagy *via* ERK-mTOR pathway

Dan Zhang, Song Han, Shizun Wang, Yanlin Luo, Li Zhao \* , Junfa Li \* 

Department of Neurobiology and Center of Stroke, Beijing Institute for Brain Disorders, Capital Medical University, Beijing, China

Received: January 16, 2017; Accepted: May 14, 2017

## Abstract

Stroke is one of the leading causes of death in the world, but its underlying mechanisms remain unclear. Both conventional protein kinase C (cPKC)  $\gamma$  and ubiquitin C-terminal hydrolase L1 (UCHL1) are neuron-specific proteins. In the models of 1-hr middle cerebral artery occlusion (MCAO)/24-hr reperfusion in mice and 1-hr oxygen–glucose deprivation (OGD)/24-hr reoxygenation in cortical neurons, we found that cPKC $\gamma$  gene knockout remarkably aggravated ischaemic injuries and simultaneously increased the levels of cleaved (Cl)-caspase-3 and LC3-I proteolysis product LC3-II, and the ratio of TUNEL-positive cells to total neurons. Moreover, cPKC $\gamma$  gene knockout could increase UCHL1 protein expression *via* elevating its mRNA level regulated by the nuclear factor  $\kappa$ B inhibitor alpha (I $\kappa$ B- $\alpha$ )/nuclear factor  $\kappa$ B (NF- $\kappa$ B) pathway in cortical neurons. Both inhibitor and shRNA of UCHL1 significantly reduced the ratio of LC3-II/total LC3, which contributed to neuronal survival after ischaemic stroke, but did not alter the level of Cl-caspase-3. In addition, UCHL1 shRNA reversed the effect of cPKC $\gamma$  on the phosphorylation levels of mTOR and ERK rather than that of AMPK and GSK-3 $\beta$ . In conclusion, our results suggest that cPKC $\gamma$  activation alleviates ischaemic injuries of mice and cortical neurons through inhibiting UCHL1 expression, which may negatively regulate autophagy through ERK-mTOR pathway.

**Keywords:** ischaemic stroke • conventional protein kinase C (cPKC) $\gamma$  • ubiquitin C-terminal hydrolase L1 • autophagy • mammalian target of rapamycin • extracellular signal-regulated kinase

## Introduction

As we all known, ischaemic stroke has high incidence and prevalence with poor outcome [1, 2]. Because of a lack of effective therapeutic treatment for ischaemic stroke, much interest is focused on understanding of molecular mechanism underlying endogenous neuroprotection against cerebral ischaemic injury. Recently, cPKC $\gamma$  in mediating stroke injury has received particular attention. cPKC $\gamma$  is expressed in the spinal cord and brain as well as exclusively localized in neurons. A noticeable increase in cPKC $\gamma$  expression is found in the ischaemic penumbra of patients with stroke [3]. The cPKC $\gamma$  membrane translocation (activation) significantly increases under the conditions of MCAO and OGD, suggesting it is involved in a conserved ischaemic response pathway [4, 5]. However, the role of cPKC $\gamma$  in cerebral ischaemic injury has not been defined unequivocally. The activation of cPKC $\gamma$  is involved in the neuroprotective effects induced by insulin and oestrogen during MCAO ischaemic injury [6, 7]. Our previous studies have shown that cPKC $\gamma$  may participate in hypoxic

preconditioning (HPC)-induced neuroprotection against cerebral ischaemic injury of BALB/c mice [8–10]. However, some studies have reported that cPKC $\gamma$  activation may exacerbate the cerebral ischaemic injuries. Down-regulation of cPKC $\gamma$  membrane translocation by its inhibitor can inhibit the increment in lactate dehydrogenase (LDH) leakage induced by 20-min. OGD treatment and decrease the decapitation-induced ischaemic brain injury of C57Bl/6J mice [5, 11]. The different effects of cPKC $\gamma$  may be attributable to the use of different species, models, protocols, measured end-points and inhibitors. In this study, using cPKC $\gamma$  gene knockout mice, we tried to further validate the role of cPKC $\gamma$  in the cerebral ischaemia-induced injury induced by 1-hr MCAO/24-hr reperfusion (R) or 1-hr OGD/24-hr reoxygenation (R) treatment.

Our previous study has identified 23 cPKC $\gamma$ -interacting proteins in the cortex of HPC-treated mice using proteomic analysis, including ubiquitin carboxy-terminal hydrolase L1 (UCHL1) [12]. UCHL1, also

\*Correspondence to: Li ZHAO, M.D.  
E-mail: zhaoli@ccmu.edu.cn

Junfa LI, Ph.D.  
E-mail: junfali@ccmu.edu.cn

known as neuronal-specific protein gene product 9.5 (PGP 9.5), is present in almost all neurons and represents 1–5% of total soluble brain protein [13]. It functions as a deubiquitinating enzyme [14], a ubiquitin (Ub) ligase [15] and a mono-Ub stabilizer [16]. Thus, its roles in neuronal cell function/dysfunction have been reported in neurodegenerative diseases, such as Alzheimer's disease (AD), Parkinson's disease (PD) and Huntington's disease (HD) [17–20]. UCHL1 is a small protein (24 kDa) and has a compact and almost globular shape, which may facilitate its crossing the blood–brain barrier (BBB) and stability in biofluid allowing for its detection [21]. The UCHL1 levels in cerebrospinal fluid (CSF) and serum of rats have been found to significantly increase after 2-hr or 6-hr MCAO, but remain normal after haemorrhagic stroke, which indicate that UCHL1 may be a vital biomarker for cerebral ischaemia injury [22, 23]. However, how UCHL1 participates in the ischaemic neuronal injuries and whether cPKC $\gamma$  regulates UCHL1 expression still remain unclear. In this study, the roles of UCHL1 mediated by cPKC $\gamma$  in the ischaemic neuronal injuries were explored *in vivo* and *in vitro*.

## Materials and methods

### Animals

The C57BL/6J wild-type (cPKC $\gamma^{+/+}$ ) and cPKC $\gamma$  knockout (cPKC $\gamma^{-/-}$ ) mice were purchased from the Jackson Laboratory (Bar Harbor, ME, USA). The experimental procedures were carried out in accordance with the recommendations in the Guide for the Care and Use of Laboratory Animals of the National Institutes of Health and approved by the experimental animal ethics committee of Capital Medical University (Permit Number: 2012-X-7). The mice were housed in the home cage under a 12:12-hr light/dark cycle, with food and water available *ad libitum* throughout the study.

Experiments were performed at room temperature (20–22°C) on male mice (6–8 W, 18–22 g). All surgeries were performed under sodium pentobarbital anaesthesia, and all efforts were made to minimize suffering. Animals were randomly divided into three groups, namely Naïve group (no treatment), Sham group (no MCAO treatment) and MCAO group (1-hr MCAO/24-hr R treatment). The MCAO-induced ischaemic stroke mouse model was performed as previous reports [24, 25]. Briefly, a 5–0 surgical nylon monofilament with its tip (0.22 ± 0.01 mm in diameter) rounded by heat (#1622-A, Shadong Biotechnology Company, Beijing, China) was gently inserted into the internal carotid artery through the external carotid artery to occlude the middle cerebral artery (MCA, a point approximately 12 mm distal to the carotid bifurcation). After 1-hr occlusion of the left MCA, the surgical nylon monofilament was carefully removed to restore blood flow and the mice were kept for 24 hrs. In the Sham group, the mice received the same surgical procedures except that the MCA was not occluded. During the surgery, rectal temperature of mice was maintained at approximately 37°C using a heating pad and an overhead lamp.

The cerebral blood flow (CBF) of the MCA supplied area was measured by laser Doppler flowmetry (Perimed Periflux system 5000, Järfälla-Stockholm, Sweden), whose tip of the probe was fixed to the surface of skull (2 mm posterior to bregma and 6 mm lateral to midline). CBF was expressed as a percentage of the baseline.

According to neurological disability status scale (NDSS), neurological deficit scores were evaluated by an observer blinded to the mouse genotype and treatment at 24 hrs after 1-hr MCAO. NDSS can be divided into 11 classes from 0 (normal) to 10 (death) [26]. The neurological dysfunction of mice was examined at 24 hrs after 1-hr MCAO. The pole test was performed to assess sensory motor function of the mice, and the time which the mouse takes to descend the ground (T total) was recorded as previously reported [27]; the foot-fault test is a measure of coordination, and the criteria are assessed as the percentage of foot-fault of the paw to the total number of steps on a wire mesh [28]; the cylinder test was performed to examine the unsymmetrical use of the forearms by recording the number of contact for each forelimb, and the ratio for contralateral limb usage is calculated using the formula  $(L - R)/(L + R + \text{Both}) \times 100\%$  [29]; and the handedness of mice was determined preference for using the paw and the criteria are shown as Laterality Index [30]. The mice were trained 3 days before MCAO surgery, meanwhile all training and tests were performed in triplicates each day. The number of mice in each group was 12; half of them were randomly chosen to measure the infarct volume by TTC staining and the others to analyse protein expression using Western blot analysis.

### Measurement of infarct volume by TTC staining

The brains of mice were cut into coronal sections about 1.5 mm thick. The slices were incubated for 15 min. in 2% 2, 3, 5-triphenyltetrazolium chloride (TTC) (Sigma-Aldrich, St. Louise, MO 63103, USA) solution at 37°C and then scanned into the computer. The photographs were analysed using Image Pro Plus 6.0 (Media Cybernetics, Silver Spring, MD, USA) according to previous report [31]. The cerebral oedema rate is given by the equation:  $(S) = (\sum LT - \sum RT)/(\sum LT + \sum RT) \times 100\%$  where  $\sum LT$  and  $\sum RT$  represent the volume of left (ischaemic) and right (non-ischaemic) hemisphere, respectively. Background (B) = volume of TTC unstained white matter in Sham group/total brain volume of Sham group  $\times 100\%$ . To eliminate the interference of oedema rate and background, the infarct rate was evaluated by this equation:  $I = \sum SIN(1 - S)/(\sum LT + \sum RT)(1 - B) \times 100\%$ ,  $\sum SIN(1 - S)$  represents the total infarct volume after deducting oedema rate.

### Primary cortical neuron culture

The primarily cultured cortical neurons were prepared from postnatal 24-hr C57BL/6J (cPKC $\gamma^{+/+}$  and cPKC $\gamma^{-/-}$ ) mice. The cortical neurons were dissociated carefully and seeded at a density of  $1.2 \times 10^5$  cells per well of 6-well plates in the DMEM medium (Gibco Inc., Grand island, NY, USA) which was replaced by the serum-free neurobasal medium (Gibco Inc.) with 2% B27 supplement (Gibco Inc.). And the culture medium was subsequently replaced half of fresh medium every 3 days.

The cortical neurons were subjected to 1-hr OGD/24-hr R to mimic ischaemic injury *in vitro*. Briefly, the neurons were replaced with glucose-free DMEM media (Gibco Inc.) and placed in the hypoxia incubator (Thermo Scientific, Marietta, OH, USA) under the condition of 5% CO $_2$ /2% O $_2$ /93% N $_2$  at 37°C. LDN-57444 (LDN) (1.0, 5.0, 10.0 or 15.0  $\mu$ M, S7135, Selleck Chemicals, Houston, TX, USA), MG-132 (5.0  $\mu$ M, S2619, Selleck Chemicals) or Bafilomycin A1 (BafA1) (100.0 nM, B1793, MO, USA) was simultaneously added into the medium, respectively.

After 1-hr OGD exposure, cells were returned to regular neurobasal medium containing 2% B27 under normoxic conditions (5% CO $_2$ /21% O $_2$ /74% N $_2$ ) for 24-hr R. After 24-hr R, cells were collected for the

following experiments. Cell viability was measured using the CellTiter 96<sup>®</sup> Aqueous One Solution Cell Proliferation Assay kit (Promega, #G3580, Madison, WI, USA), and cell death was determined via LDH release rate using the CytoTox 96<sup>®</sup> Non-Radioactive Cytotoxicity Assay kit (Promega, #G1780) following the manufacturer's instructions.

## Lentiviral transduction

The neurons were transduced with lentiviral vectors containing UCHL1 shRNA gene (LV3-GFP-UCHL1 shRNA 1#, 5'-GAAACTCCTGTGGTAC-CATCG-3'; LV3-GFP-UCHL1 shRNA 2#, 5'-GAAGATAGAGCCAAGTGTTC-3'; LV3-GFP-UCHL1 shRNA 3#, 5'-GGGTAGATGACAAA GTGAATT-3'; LV3-GFP-UCHL1 shRNA 4#, 5'-GCTGTCTTCTTGGCTTCTACA-3') or the negative control (NC) (LV3-GFP-CN, 5'-TTCTCCGAACGTGTACGT-3') according to the manufacturer's instruction (Sangon Biotech, Shanghai, China) after 3 days of culture. The efficiency of transducing the lentiviral vectors into primary culture of neurons was about 70%. After 72-hr lentiviral transduction, the neurons were subjected to 1-hr OGD/24-hr R treatment.

## Western blot analysis

As previously reported [32], total protein of the tissues from peri-infarct region or cultured cortical neurons were extracted by lysis buffer. The samples (30 µg) were subjected to 10% or 12% SDS-PAGE and transferred onto polyvinylidene difluoride membrane (GE Healthcare, Buckinghamshire, UK). The membranes were incubated at 4°C overnight in the solution consisting of primary antibodies against cPKC $\gamma$  (1:1000, sc-211, Santa Cruz Biotechnology, Heidelberg, Germany), nuclear factor  $\kappa$ B inhibitor alpha ( $\text{I}\kappa\text{B-}\alpha$ ) (1:500, sc-371, Santa Cruz Biotechnology), phospho-I $\kappa\text{B-}\alpha$  (Ser 32, 1:250, sc-7977, Santa Cruz Biotechnology), adenosine 5'-monophosphate-activated protein kinase (AMPK) (1:1000, #07-350, Millipore, St. Louis, MA, USA), extracellular signal-regulated kinase (ERK) (1:10000, #06-182, Millipore, St. Louis, MA, USA), UCHL1 (1:1000, #13179, Cell Signaling Technology, Beverly, MA, USA), caspase-3 (1:1000, #9665, Cell Signaling Technology), LC3 (1:1000, #12741, Cell Signaling Technology), mammalian target of rapamycin (mTOR) (1:400, #2972, Cell Signaling Technology), phospho-mTOR (Ser2448, 1:250, #2971, Cell Signaling Technology), phospho-ERK (1:1000, #9101, Cell Signaling Technology), phospho-AMPK (Thr172, 1:500, #2535, Cell Signaling Technology), glycogen synthase kinase-3 (GSK-3) $\beta$  (1:1000, #9315, Cell Signaling Technology), phospho-GSK-3 $\beta$  (Ser9, 1:1000, Cell Signaling Technology),  $\beta$ -actin (1:10000, #60008-1-Ig, Proteintech, Rosemont, IL, USA) and  $\beta$ -tubulin (1:10000, T2200, Sigma-Aldrich). Horseradish peroxidase-conjugated goat anti-rabbit or antimouse IgG was used as secondary antibodies (1:4000; Jackson Immuno Research, West Grove, PA, USA) for 1 hr at room temperature. Then the SuperSignal<sup>®</sup> West Pico Chemiluminescent Substrate (#NCI5080, Thermo Fisher Scientific, Waltham, MA, USA) was employed to detect the signals. The amount of proteins were quantified by densitometry and normalized to  $\beta$ -actin or  $\beta$ -tubulin, an internal standard.

## Sandwich ELISA

The CSF and serum of mice after 1-hr MCAO/24-hr R and the medium of the cultured cortical neurons after 1-hr OGD/24-hr R were collected and measured by a commercial enzyme-linked immunosorbent assay (ELISA) kit (Abnova, #KA3378, Taiwan, China). Experimental procedures were

performed according to the manufacturer's protocol. Each sample was measured in duplicate. Optical densities were determined with a microplate reader set to dual wavelengths of 450 nm/540 nm. Standard curves were generated using recombinant UCHL1 proteins in a different dilution series.

## RNA isolation and real-time quantitative RT-PCR

Total RNA was isolated from cultured cortical neurons with the RNeasy Lipid Tissue Mini Kit (QIAGEN, #74804, Germantown, MD, USA) according to the manufacturer's instruction. The RNA was used to generate cDNA by Maxima First Strand cDNA Synthesis Kit for real-time quantitative RT-PCR (Thermo Fisher Scientific, #K1642) according to the manufacturer's instructions. To detect UCHL1 expression, the 3'-untranslated region (NM\_011670.2, bp 336–545) was amplified with a forward primer: 5'-CGGCCAGCATGAAAACCTC-3' and a reverse primer: 5'-GGGACAGCTTCTCCGTTTCA-3'. Equal amounts of cDNA were used for real-time quantitative RT-PCR analysis using the Power SYBR<sup>®</sup> Green PCR Master Mix (Applied Biosystems, #4367659, Carlsbad, CA, USA) according to the manufacturer's instructions. Fluorescent products were detected using a 7500 real-time PCR thermal cycler (Applied Biosystems). Ywazh (forward primer: 5'-AGAGTCGTACAAGACAGCAC-3' and reverse primer: 5'-GAATGAGGCAGACA AAGGTTG-3') was used as an internal control [33]. Then the relative expression level was calculated using the following equation: relative gene expression =  $2^{-(\Delta\text{Ct sample} - \Delta\text{Ct control})}$  [34].

## Immunofluorescent staining

The TUNEL staining assay using the *In Situ* Cell Death Detection Kit (Roche, #11684817910, Berlin, Germany) was performed following the manufacturer's protocol. Briefly, the primarily cultured cortical neurons were fixed with 4% paraformaldehyde at room temperature. This was followed by incubating in a permeabilization solution and then incubating with a TUNEL reaction mixture. For the following immunofluorescent staining, fixed cells were incubated with antibody for NeuN to identify neuron (1:500, #ab104224, Abcam, Cambridge, MA, USA) and antibody for glial fibrillary acidic protein to identify astrocyte (GFAP, 1:1000, #Z0334, Dako Denmark A/S, Glostrup, Denmark) at 4°C overnight followed by TUNEL staining. Then cells were exposed to Alexa 594-conjugated goat anti-mouse secondary antibody (1:500, Invitrogen, Eugene, OR, USA) and Alexa 350-conjugated goat anti-rabbit secondary antibody (1:500, Invitrogen, Eugene, OR, USA) for 1 hr at 37°C in a dark chamber, respectively. The images were captured by a fluorescence microscope, and data were expressed as the ratio of TUNEL-positive cells to total neurons.

## Statistical analysis

The protein expression levels of cPKC $\gamma$  and UCHL1 (the band density of target protein/ $\beta$ -actin or  $\beta$ -tubulin), the phosphorylation levels of mTOR, ERK, AMPK and GSK-3 $\beta$  (the band density of phosphorylated form/total protein), the proteolysis levels of caspases (band density of cleaved caspase/total caspase), the ratio of TUNEL-positive neurons and LC3-II (band density of LC3-II/band density of LC3-I and II) were calculated as 100% in the control group (Naïve *in vivo*/Normoxia *in vitro*), and then the other groups were expressed as percentage of that of control group. Neurological deficits data were analysed using the nonparametric Kruskal–Wallis test. The values were presented as mean  $\pm$  S.E.M. Statistical analysis was performed using one-way analysis of variance (ANOVA) followed by all

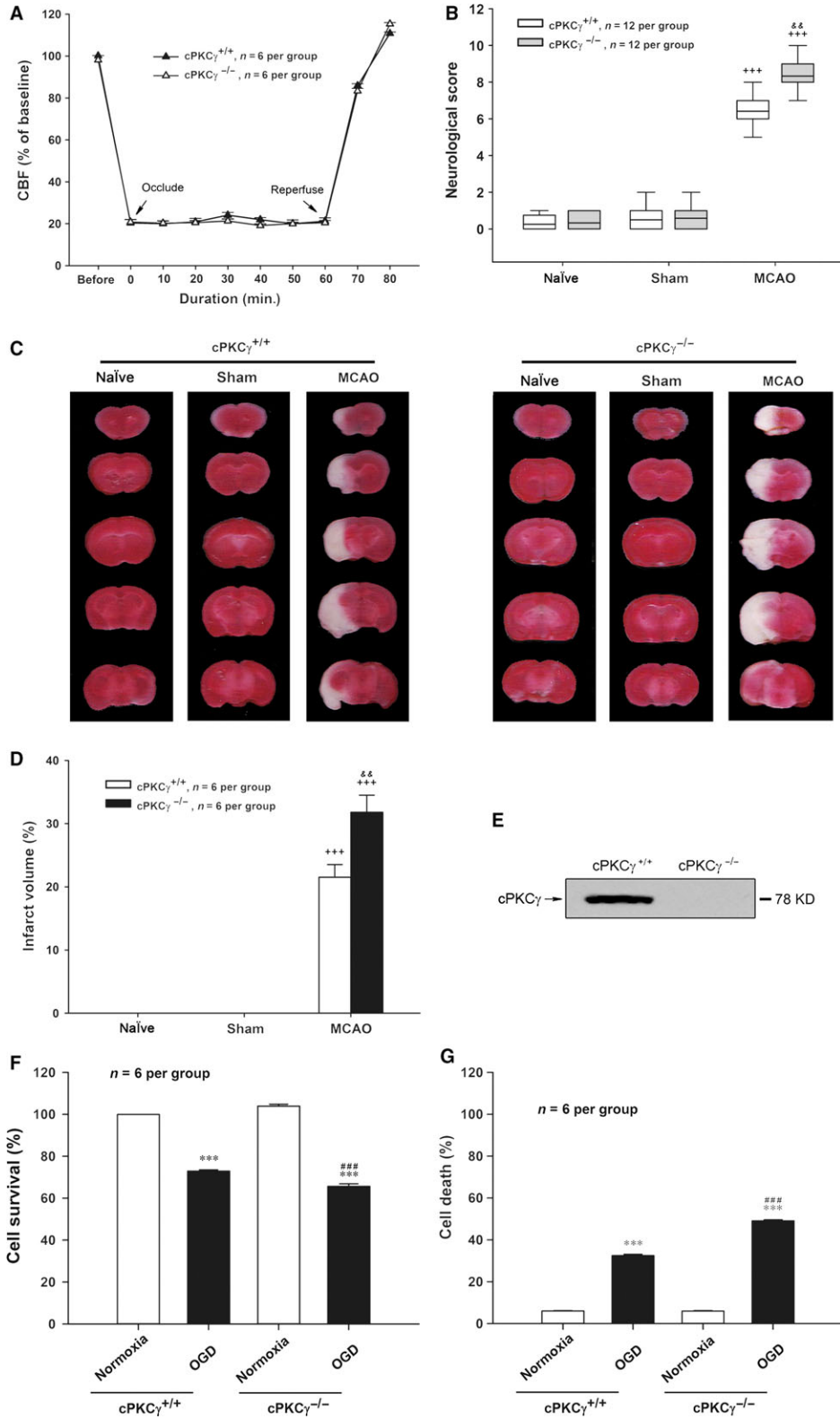


**Fig. 1** Effects of cPKC $\gamma$  on regional CBF, neurological score and infarct volume of mice after 1-hr MCAO/24-hr R, and cell survival and death rates of cultured cortical neurons after 1-hr OGD/24-hr R. **(A)** The change in CBF of mice with MCAO treatment ( $n = 6$  per group). **(B)** Statistical results of neurological score ( $n = 12$  per group). Representative photographs of TTC-stained coronal brain sections **(C)** and statistical results of infarct volume **(D)** from Naïve, Sham and MCAO groups of cPKC $\gamma^{+/+}$  and cPKC $\gamma^{-/-}$  mice ( $n = 6$  per group), respectively. **(E)** Representative results of Western blot demonstrated that cPKC $\gamma$  was completely knocked out in mice. Quantitative analysis of the cell survival rate **(F)** and the cell death rate **(G)** from Normoxia and OGD groups of cPKC $\gamma^{+/+}$  and cPKC $\gamma^{-/-}$  cortical neurons ( $n = 6$  per group), respectively.  $^{+++}P < 0.001$  versus Sham of cPKC $\gamma^{+/+}$  mice;  $^{\&\&}P < 0.01$  versus corresponding cPKC $\gamma^{+/+}$  mice with the same treatment;  $^{***}P < 0.001$  versus Normoxia of cPKC $\gamma^{+/+}$  neurons;  $^{###}P < 0.001$  versus corresponding cPKC $\gamma^{+/+}$  cortical neurons with the same treatment.

pairwise multiple comparison procedures using Bonferroni test and  $P < 0.05$  was considered as statistically significance.

## Results

### cPKC $\gamma$ could attenuate ischaemic injuries induced by MCAO or OGD treatment

To figure out whether cPKC $\gamma$  acted as a protective or deleterious molecule during cerebral ischaemic injuries, the regional CBF,

neurological deficits and infarct volume were assessed after 1-hr MCAO/24-hr R, and the cell survival and death rates were tested after 1-hr OGD/24-hr R. cPKC $\gamma$  was completely knocked out in mice (Fig. 1 E). We found that the regional CBF sharply reduced to about 20% of baseline value after the onset of MCAO and recovered completely after removing the surgical nylon monofilament (Fig. 1A,  $n = 6$  per group). There were no significant differences between cPKC $\gamma^{+/+}$  and cPKC $\gamma^{-/-}$  mice, indicating that cPKC $\gamma$  did not affect CBF level during the procedure of 1-hr MCAO/24-hr R treatment (Fig. 1A,  $n = 6$  per group). We observed that there were no neurological deficits and infarction in the Naïve and Sham groups. The neurological score and infarct volume remarkably increased after 1-hr MCAO/24-hr R and further

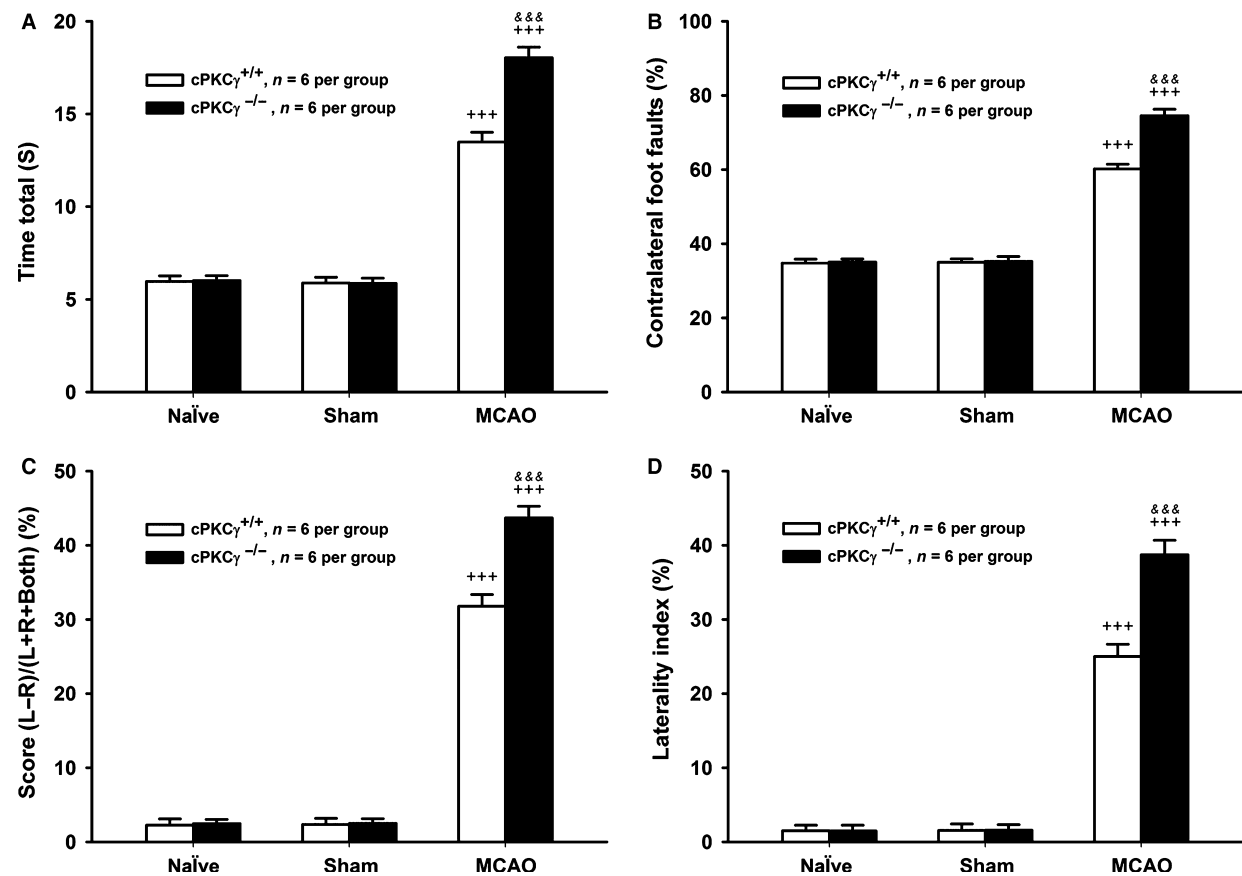


**Fig. 2** Effects of cPKC $\gamma$  on the neurological outcome of mice after 1-hr MCAO/24-hr R. Statistical results of pole test **(A)**, foot-fault test **(B)**, cylinder test **(C)** and handedness test **(D)** from Naïve, Sham and MCAO groups of cPKC $\gamma^{+/+}$  and cPKC $\gamma^{-/-}$  mice ( $n = 6$  per group), respectively.  $^{+++}P < 0.001$  versus Sham of cPKC $\gamma^{+/+}$  mice;  $^{\&\&\&}P < 0.01$  versus corresponding cPKC $\gamma^{+/+}$  mice with the same treatment.

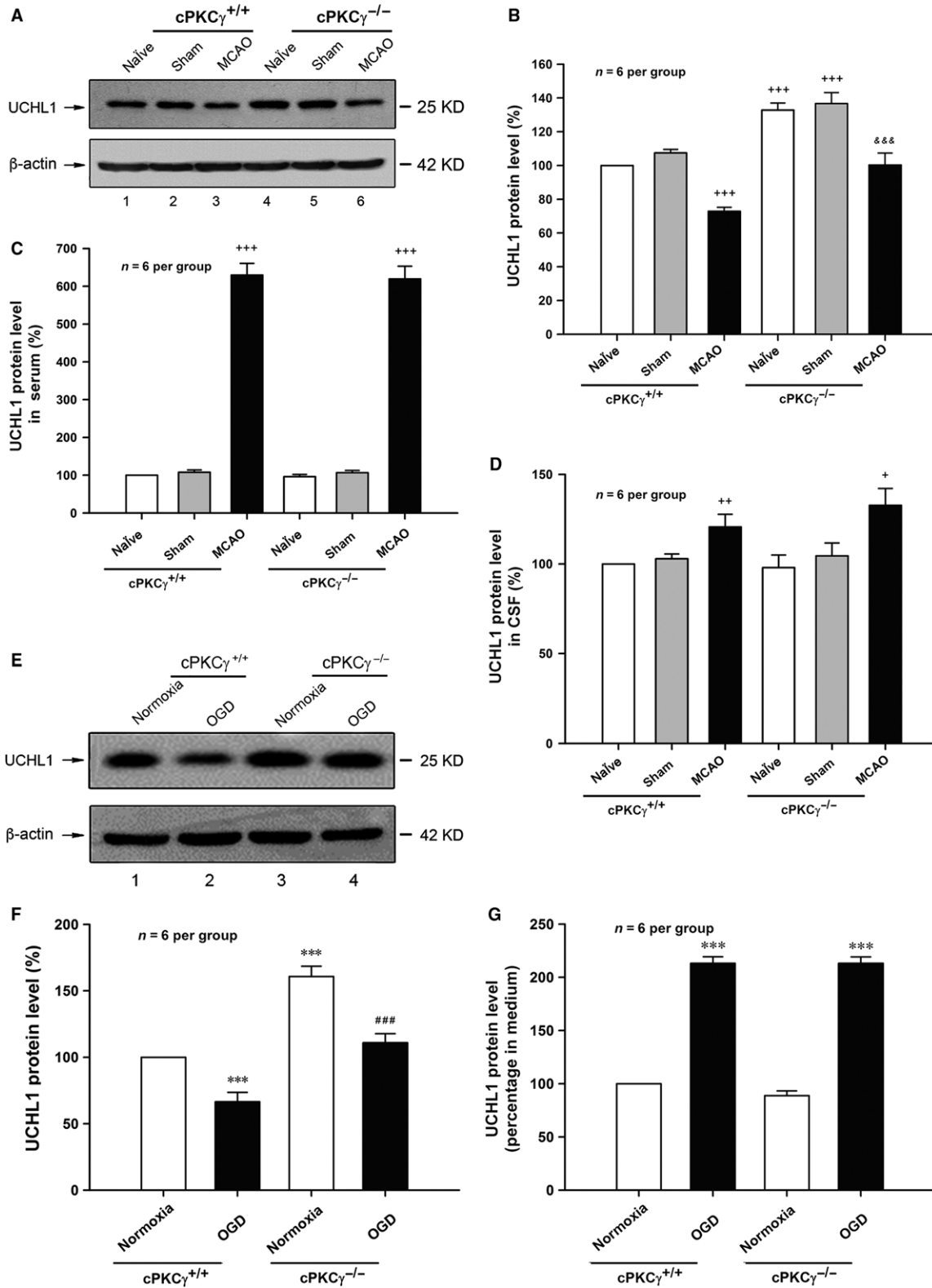




**Fig. 3** Effects of cPKC $\gamma$  on the level of UCHL1 after 1-hr MCAO/24-hr R and 1-hr OGD/24-hr R. Representative results (A) and quantitative analysis (B) of Western blot showed the changes in UCHL1 level in the cortex from Naïve, Sham and MCAO groups of cPKC $\gamma^{+/+}$  and cPKC $\gamma^{-/-}$  mice ( $n = 6$  per group), respectively. Statistical results of UCHL1 level in serum (C) and CSF (D) from Naïve, Sham and MCAO groups of cPKC $\gamma^{+/+}$  and cPKC $\gamma^{-/-}$  mice ( $n = 6$  per group), respectively. Representative results (E) and quantitative analysis (F) of Western blot showed the changes in UCHL1 level from Normoxia and OGD groups of cPKC $\gamma^{+/+}$  and cPKC $\gamma^{-/-}$  cortical neurons ( $n = 6$  per group), respectively. (G) Statistical results of UCHL1 level in medium from Normoxia and OGD groups of cPKC $\gamma^{+/+}$  and cPKC $\gamma^{-/-}$  cortical neurons ( $n = 6$  per group), respectively. \* $P < 0.05$ , \*\* $P < 0.01$ , \*\*\* $P < 0.001$  versus Sham of cPKC $\gamma^{+/+}$  mice; &&& $P < 0.001$  versus corresponding cPKC $\gamma^{+/+}$  mice with the same treatment; \*\*\* $P < 0.001$  versus Normoxia of cPKC $\gamma^{+/+}$  neurons; ### $P < 0.001$  versus corresponding cPKC $\gamma^{+/+}$  cortical neurons with the same treatment.

increased in cPKC $\gamma^{-/-}$  mice compared with that of cPKC $\gamma^{+/+}$  mice, respectively (Fig. 1B,  $P < 0.001$ ,  $P < 0.01$ ,  $n = 12$  per group; Fig. 1C and D,  $P < 0.001$ ,  $P < 0.01$ ,  $n = 6$  per group). Meanwhile, results of pole test (Fig. 2A), foot-fault test (Fig. 2B), cylinder test (Fig. 2C) and handedness test (Fig. 2D) showed that 1-hr MCAO/24-hr R remarkably aggravated the neurological deficits of cPKC $\gamma^{-/-}$  mice compared with that of cPKC $\gamma^{+/+}$  mice ( $P < 0.001$ ,  $n = 6$  per group). In concert with these results of MCAO treatment, 1-hr OGD/24-hr R treatment significantly decreased the cell survival rate and simultaneously increased the cell death rate compared with that of Normoxia group, respectively (Fig. 1F and G,  $P < 0.001$ ,  $n = 6$  per group). Moreover, cPKC $\gamma$  gene knockout further decreased the cell survival rate and simultaneously increased the cell death rate, respectively (Fig. 1F and G,  $P < 0.001$ ,  $n = 6$  per group). These results provide further evidence that cPKC $\gamma$  may protect neurons against OGD- or MCAO-induced ischaemic injury.

### **cPKC $\gamma$ could decrease the protein expressions of UCHL1 after MCAO or OGD treatment**

In the next set of experiments, we observed whether cPKC $\gamma$  could regulate UCHL1 expression or release. Our results showed that the protein expression of UCHL1 obviously decreased, while the levels of UCHL1 in serum and CSF significantly increased after 1-hr MCAO/24-hr R (Fig. 3A-D,  $P < 0.001$ ,  $n = 6$  per group). There were no obvious differences in the levels of UCHL1 in serum and CSF between cPKC $\gamma^{+/+}$  and cPKC $\gamma^{-/-}$  mice, respectively. However, the UCHL1 protein expression significantly increased in the cPKC $\gamma^{-/-}$  mice compared with that of cPKC $\gamma^{+/+}$  mice after 1-hr MCAO/24-hr R (Fig. 3A-D,  $P < 0.001$ ,  $n = 6$  per group).

The 1-hr OGD/24-hr R treatment also led to increased level of UCHL1 in culture medium and decreased UCHL1 protein expression of primary cortical neurons (Fig. 3E-G,  $P < 0.001$ ,  $n = 6$  per group). cPKC $\gamma$  gene knockout did not change the level of UCHL1 in culture medium, but significantly increased the UCHL1 protein expression after 1-hr OGD/24-hr R treatment (Fig. 3E-G,  $P < 0.001$ ,  $n = 6$  per group). Our results indicate that cPKC $\gamma$  inhibits UCHL1 protein expression but does not affect the UCHL1 release following MCAO or OGD treatment.

### **cPKC $\gamma$ could decrease the mRNA expression of UCHL1 after OGD treatment**

To determine the cause of UCHL1 down-regulation by cPKC $\gamma$ , we observed the change in protein degradation and mRNA expression of

UCHL1 in OGD-treated neurons. Our results showed that the UCHL1 protein expression was not altered by MG-132, a proteasome inhibitor, in cPKC $\gamma^{-/-}$  neurons following 1-hr OGD/24-hr R treatment (Fig. 4A and B,  $P > 0.05$ ,  $n = 6$  per group). However, the UCHL1 mRNA expression significantly decreased in 1-hr OGD/24-hr R-treated cortical neurons and enhanced in response to cPKC $\gamma$  gene knockout using agarose gel electrophoresis and real-time quantitative RT-PCR (Fig. 4C and D,  $P < 0.001$ ,  $n = 6$  per group). Our results above indicate that cPKC $\gamma$  may decrease mRNA level of UCHL1 rather than its protein degradation.

It has been reported that the functional nuclear factor  $\kappa$ B (NF- $\kappa$ B) response element is found in the UCHL1 promoter region, and NF- $\kappa$ B activation can suppress UCHL1 gene transcription [35, 36]. NF- $\kappa$ B is activated through the phosphorylation of I $\kappa$ B- $\alpha$ . Our results showed that the phosphorylation of I $\kappa$ B- $\alpha$  on Ser-32 significantly increased after 1-hr OGD/24-hr R, but obviously decreased in response to cPKC $\gamma$  gene knockout (Fig. 4E and F,  $P < 0.001$ ,  $n = 6$  per group). These results above indicate that cPKC $\gamma$  may inhibit the mRNA level of UCHL1 via I $\kappa$ B- $\alpha$ /NF- $\kappa$ B pathway.

### **UCHL1 could aggravate the cortical neuron injuries induced by 1-hr OGD/24-hr R treatment**

To figure out the possible role of UCHL1 in OGD-induced ischaemic injuries, LDN, the UCHL1 inhibitor, was used in four different dosages of 1.0, 5.0, 10.0 and 15.0  $\mu$ M. As shown in Figure 5A and B, LDN (5, 10 and 15  $\mu$ M) significantly increased the cell survival rate and simultaneously decreased the cell death rate in the cortical neurons with 1-hr OGD/24-hr R treatment (Fig. 5A and B,  $P < 0.001$ ,  $n = 6$  per group). These results illustrate that UCHL1 may aggravate 1-hr OGD/24-hr R-induced cortical neuron injuries. Consequently, 10  $\mu$ M LDN was chosen in the following experiments.

To explore whether cPKC $\gamma$  alleviated ischaemic injury in cultured cortical neurons through inhibiting UCHL1 expression, four UCHL1 shRNA candidates were used. UCHL1 shRNA2 and 3 which more effectively inhibited UCHL1 expression (Fig. 5C) were chosen in the following experiments. As shown in Figure 5D, UCHL1 shRNA 2 and 3 treatments reversed the increased cell death rate induced by cPKC $\gamma$  gene knockout in 1-hr OGD/24-hr R-treated neurons ( $P < 0.001$ ,  $n = 6$  per group).

### **Down-regulation of UCHL1 mediated by cPKC $\gamma$ protected neurons against ischaemic stroke through autophagy**

Apoptosis and autophagy were two major morphologically distinctive forms of programmed cell death [25, 37]. To explore the role of

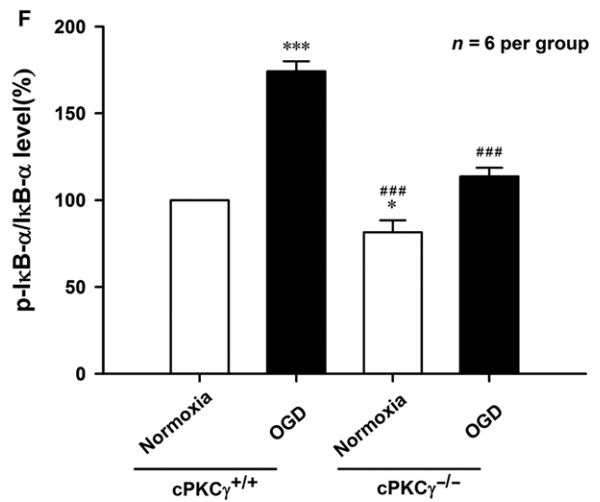
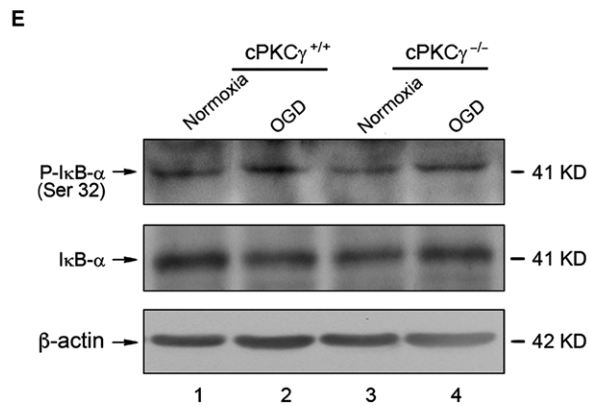
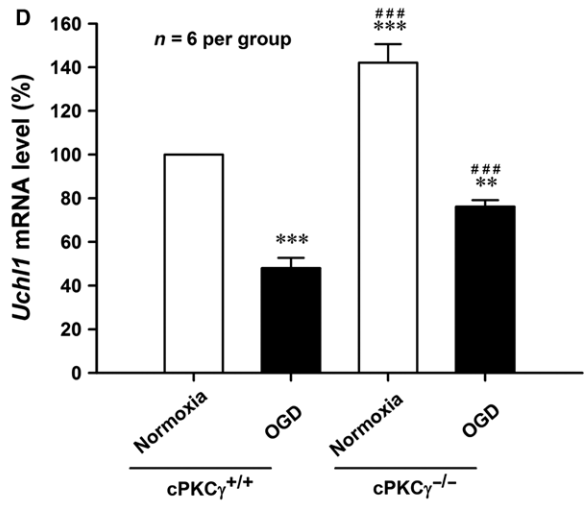
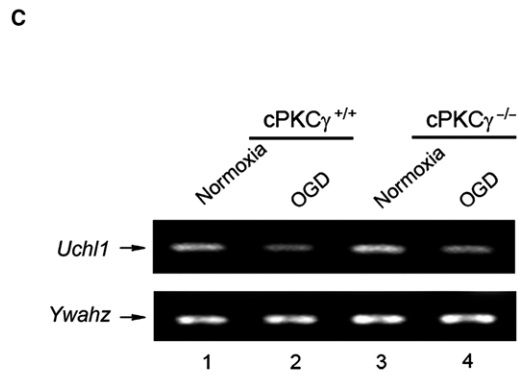
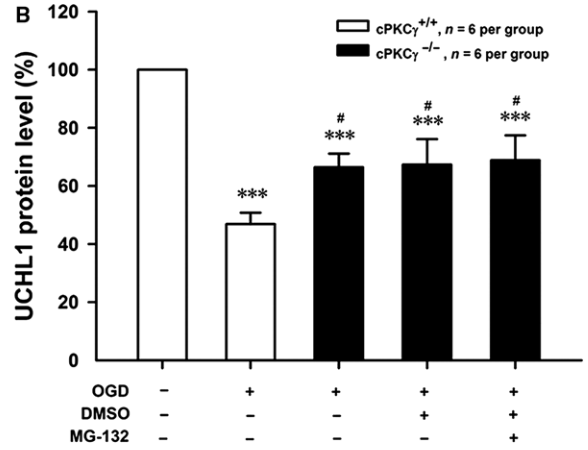
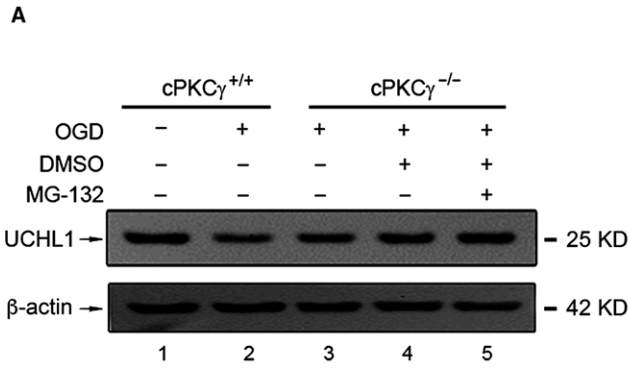




**Fig. 4** Effects of cPKC $\gamma$  on the UCHL1 protein and mRNA expression in cortical neurons after 1-hr OGD/24-hr R. Representative results (A) and quantitative analysis (B) of Western blot showed the change in UCHL1 protein expression after MG-132 (5.0  $\mu$ M) treatments ( $n = 6$  per group). Typical images of PCR (C) and quantitative analysis of real-time quantity RT-PCR (D) showed the mRNA level of UCHL1 from Normoxia and OGD groups of cPKC $\gamma^{+/+}$  and cPKC $\gamma^{-/-}$  cortical neurons ( $n = 6$  per group), respectively. Representative results (E) and statistical results (F) of Western blot showed the levels of P-I $\kappa$ B- $\alpha$  and total I $\kappa$ B- $\alpha$  from Normoxia and OGD groups of cPKC $\gamma^{+/+}$  and cPKC $\gamma^{-/-}$  cortical neurons ( $n = 6$  per group), respectively. \* $P < 0.05$ , \*\* $P < 0.01$ , \*\*\* $P < 0.001$  versus Normoxia of cPKC $\gamma^{+/+}$  neurons; # $P < 0.05$ , ### $P < 0.001$  versus corresponding cPKC $\gamma^{+/+}$  cortical neurons with the same treatment.

cPKC $\gamma$  and UCHL1 in apoptosis and autophagy induced by MCAO or OGD treatment, the ratios of cleaved/total caspase-3, the TUNEL staining assay and LC3-II/total LC3 were detected. We found that the ratio of cleaved/total caspase-3 significantly increased after 1-hr OGD/24-hr R and further increased in cPKC $\gamma^{-/-}$  neuron compared with that of cPKC $\gamma^{+/+}$  neuron (Fig. 6A and B,  $P < 0.05$ ,  $n = 6$  per group; Fig. 6C and D,  $P < 0.01$ ,  $n = 6$  per group), but was not altered

by LDN or UCHL1 shRNA treatment (Fig. 6A-D,  $P > 0.05$ ,  $n = 6$  per group). The TUNEL staining assay was conducted to assess potential apoptosis; NeuN and glial fibrillary acidic protein (GFAP) were used to identify neurons and astrocytes, respectively. Consistent with the results of caspase-3, the 1-hr OGD/24-hr R treatment also led to a significant increase of the TUNEL-positive neurons in cPKC $\gamma^{-/-}$  mice compared with that of cPKC $\gamma^{+/+}$  mice, but was not altered by LDN

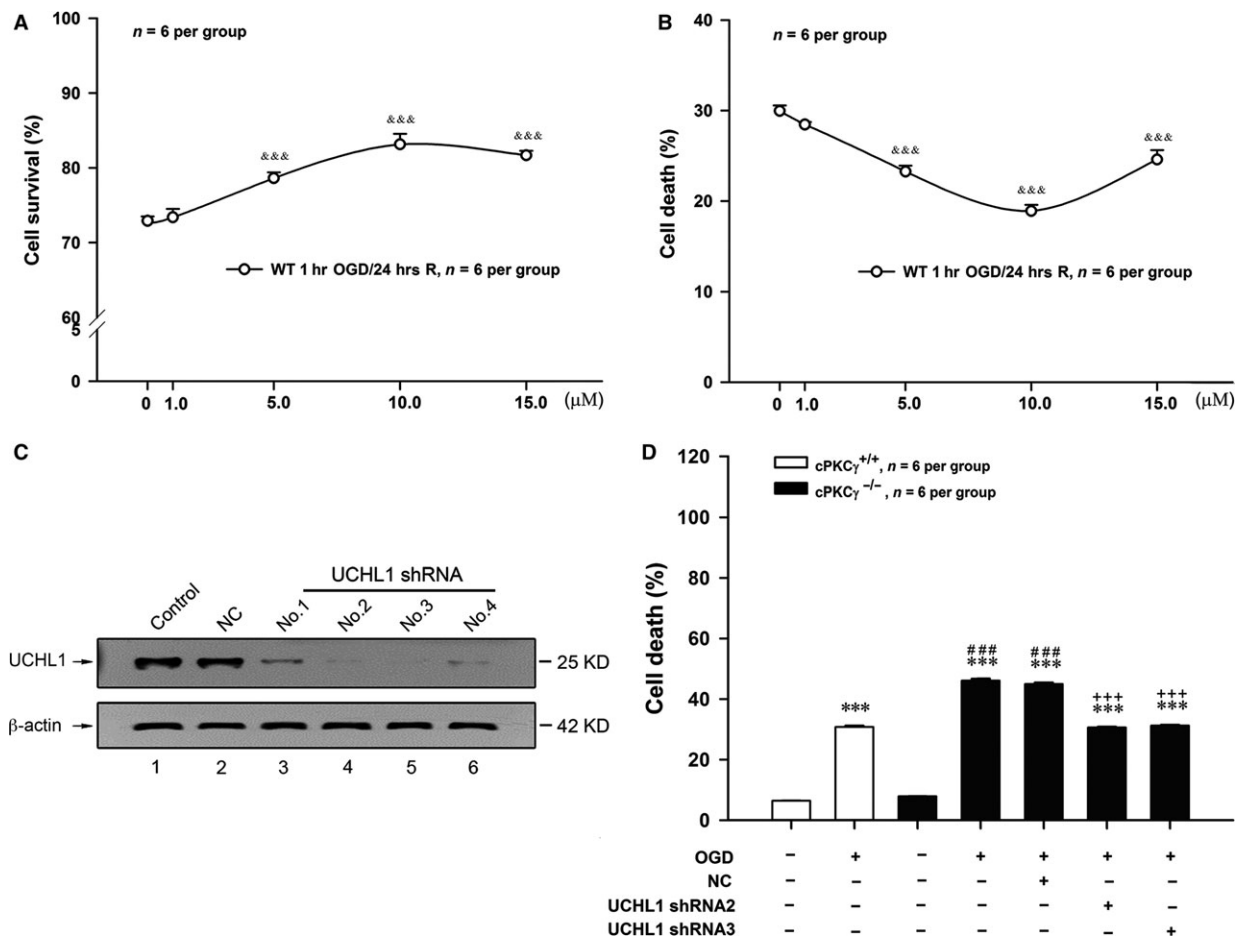


**Fig. 5** Effects of UCHL1 on the rates of cell survival and death of cultured cortical neurons after 1-hr OGD/24-hr R. Quantitative results showed the effects of different doses of LDN on the rate of cell survival (A) and the rate of cell death (B) induced by OGD treatment ( $n = 6$  per group). (C) Representative results of Western blot showed UCHL1 shRNA2 and shRNA3 could obviously decrease UCHL1 protein expression, especially. (D) Quantitative analysis showed the effects of UCHL1 shRNA2 and shRNA3 treatments on the rate of cell death from Normoxia and OGD groups of cPKC $\gamma^{+/+}$  and cPKC $\gamma^{-/-}$  cortical neurons ( $n = 6$  per group), respectively. &&& $P < 0.001$  versus vehicle of LDN group with the same treatment; \*\*\* $P < 0.001$  versus Normoxia of cPKC $\gamma^{+/+}$  neurons; ### $P < 0.001$  versus corresponding cPKC $\gamma^{+/+}$  cortical neurons with the same treatment; +++ $P < 0.001$  versus NC with the same treatment.

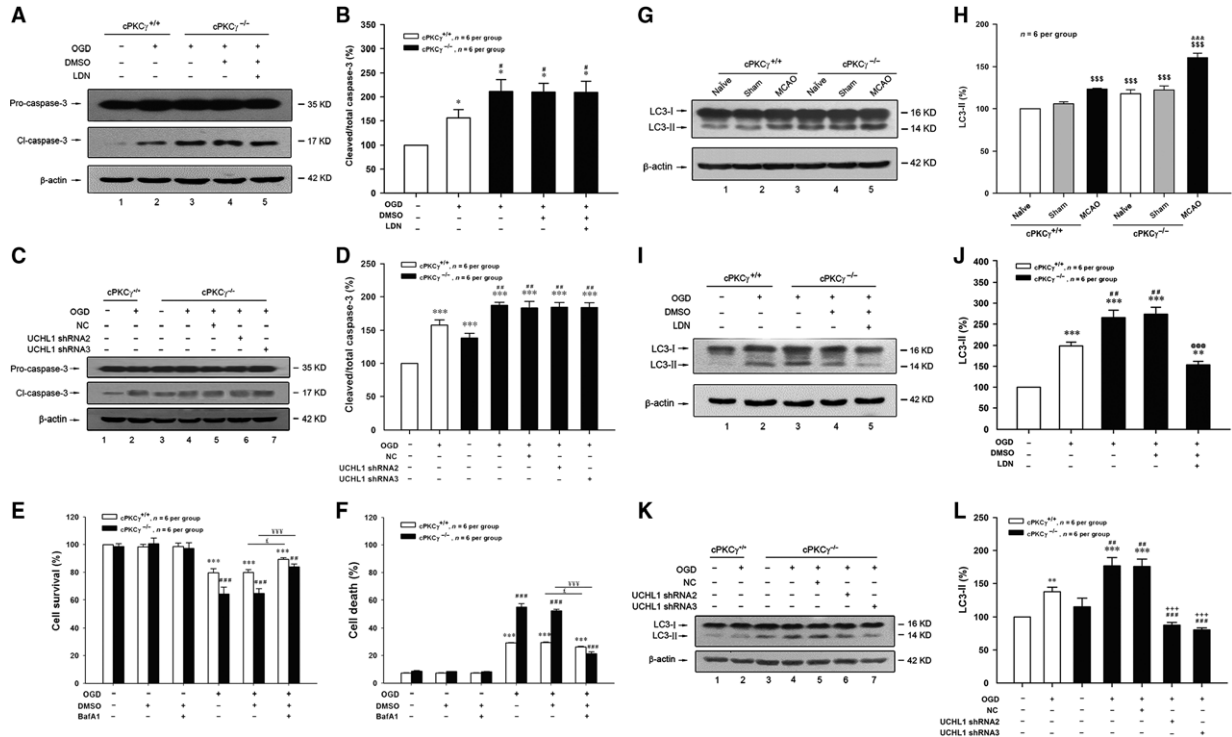


**Fig. 6** Effects of UCHL1 on the expression of caspase-3 or LC3 in cortical neurons after 1-hr MCAO/24-hr R or 1-hr OGD/24-hr R. Representative results (A and C) and quantitative analysis (B and D) of Western blot showed the effects of LDN (10.0  $\mu$ M) and UCHL1 shRNA treatments on the expressions of Pro-caspase-3 and Cl-caspase-3 from Normoxia and OGD groups of cPKC $\gamma^{+/+}$  and cPKC $\gamma^{-/-}$  cortical neurons ( $n = 6$  per group), respectively. Quantitative results showed the effects of autophagy inhibitor BafA1 (100.0 nM) on the rate of cell survival (E) and the rate of cell death (F) from Normoxia and OGD groups of cPKC $\gamma^{+/+}$  and cPKC $\gamma^{-/-}$  cortical neurons ( $n = 6$  per group), respectively. Representative result (G) and quantitative analysis (H) of Western blot showed the expression of LC3-I and LC3-II in the cortex from Naive, Sham and MCAO groups of cPKC $\gamma^{+/+}$  and cPKC $\gamma^{-/-}$  mice ( $n = 6$  per group), respectively. Representative results (I and K) and quantitative analysis (J and L) of Western blot showed the effects of LDN (10.0  $\mu$ M) and UCHL1 shRNA treatments on the expressions of LC3-II and LC3-I from Normoxia and OGD groups of cPKC $\gamma^{+/+}$  and cPKC $\gamma^{-/-}$  cortical neurons ( $n = 6$  per group), respectively. \*\*\* $P < 0.001$ , \*\* $P < 0.01$ , \* $P < 0.05$  versus Normoxia of cPKC $\gamma^{+/+}$  neurons; ### $P < 0.001$ , ## $P < 0.01$ , # $P < 0.05$  versus corresponding cPKC $\gamma^{+/+}$  cortical neurons with the same treatment;  $\xi P < 0.05$  versus OGD of cPKC $\gamma^{+/+}$  neurons without BafA1 treatment;  $\eta P < 0.001$  versus OGD of cPKC $\gamma^{-/-}$  neurons without BafA1 treatment;  $\zeta P < 0.001$  versus Naive of cPKC $\gamma^{+/+}$  mice;  $\omega P < 0.001$  versus corresponding cPKC $\gamma^{+/+}$  mice with the same treatment; @ $P < 0.001$  versus vehicle of LDN group with the same treatment; +++ $P < 0.001$  versus NC with the same treatment.

treatment (Fig. 7A and B,  $P < 0.001$ ,  $n = 6$  per group). These results suggest that UCHL1 does not involve in the effect of cPKC $\gamma$  on neuronal apoptosis.

Moreover, the conversion of LC3-I to LC3-II evidently increased after 1-hr OGD/24-hr R or 1-hr MCAO/24-hr R treatments (Fig. 6G and H,  $P < 0.001$ ,  $n = 6$  per group; Fig. 6I and J,  $P < 0.001$ ,  $n = 6$  per group; Fig. 6K and L,  $P < 0.01$ ,  $n = 6$  per group). The role of autophagy in ischaemic stroke is still controversial. Therefore, BafA1, an autophagy inhibitor, was used to determine the role of autophagy in the ischaemic neuronal injury. BafA1 treatment was found to increase the cell survival rate and simultaneously decrease the cell death rate in both cPKC $\gamma^{+/+}$  and cPKC $\gamma^{-/-}$  neurons after 1-hr OGD/24-hr R (Fig. 6E and F,  $P < 0.05$  or  $0.001$ ,  $n = 6$  per group), which indicate that autophagy may aggravate ischaemic neuronal injuries. The high ratio of LC3-II/total LC3 induced by MCAO or OGD treatment was further increased by cPKC $\gamma$  gene knockout and then was

significantly decreased by LDN or UCHL1 shRNA treatment (Fig. 6G and H,  $P < 0.001$ ,  $n = 6$  per group; Fig. 6I-L,  $P < 0.01$ ,  $n = 6$  per group). Our results demonstrate that down-regulation of UCHL1 might involve in the effect of cPKC $\gamma$  on autophagy during ischaemic injury.

### Down-regulation of UCHL1 mediated by cPKC $\gamma$ decreased OGD-induced autophagy through ERK-mTOR pathway

To explore the roles of cPKC $\gamma$  and UCHL1 in OGD-induced autophagy *in vitro*, the autophagy-related protein expressions were observed. Our results showed that 1-hr OGD/24-hr R treatment could obviously reduce mTOR phosphorylation (P-mTOR) and cPKC $\gamma$  gene knockout resulted in more reduction in P-mTOR (Fig. 8A and B,  $P < 0.01$ ,

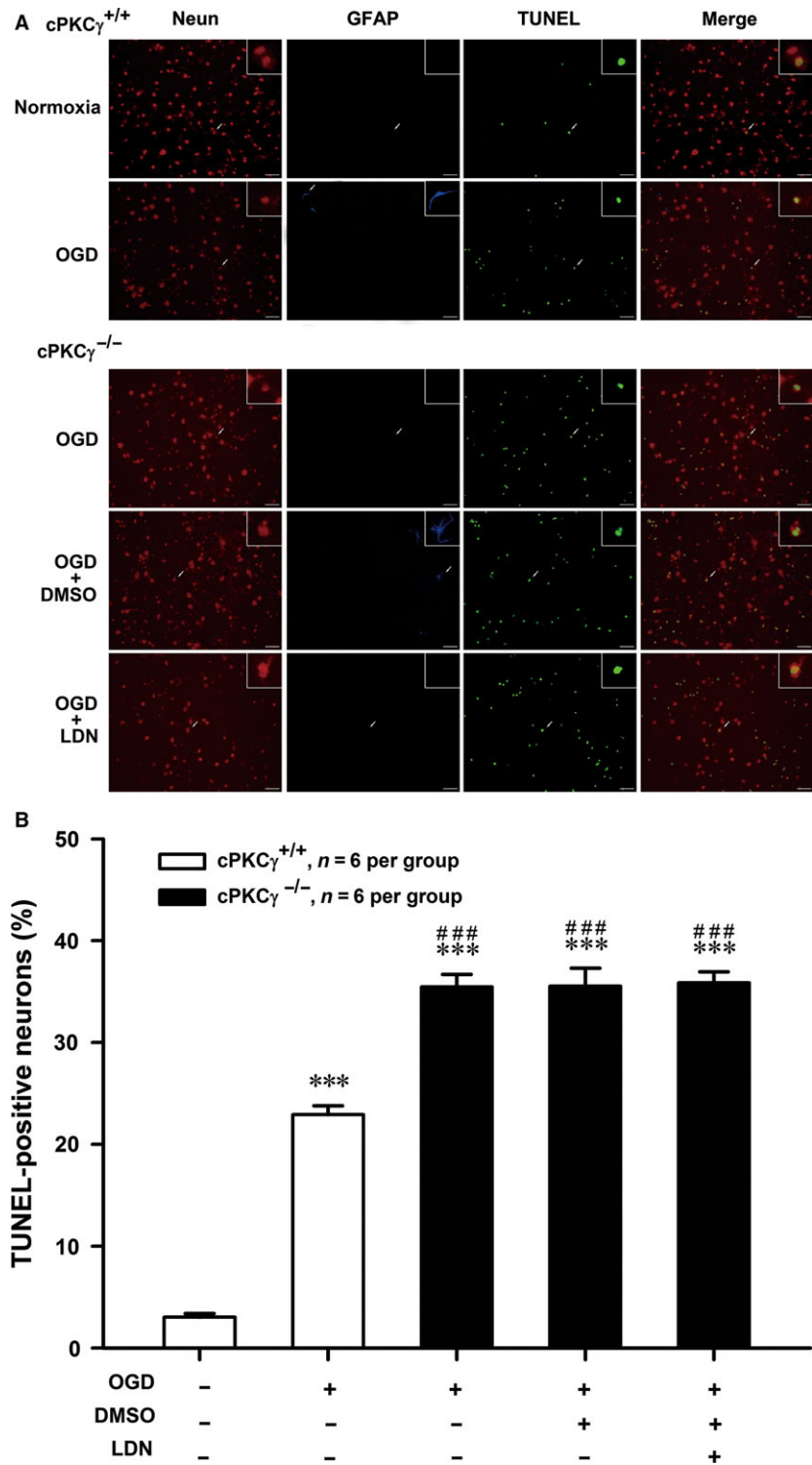


**Fig. 7** Effects of UCHL1 on the level of TUNEL-positive neurons in cortical neurons after 1-hr OGD/24-hr R. Merged images (A) of NeuN (red), GFAP (blue) and TUNEL (green) and quantitative analysis (B) showed the effects of LDN (10.0  $\mu$ M) on the level of TUNEL-positive neurons from Normoxia and OGD groups of  $cPKC\gamma^{+/+}$  and  $cPKC\gamma^{-/-}$  cortical neurons ( $n = 6$  per group), respectively. \*\*\* $P < 0.001$  versus Normoxia of  $cPKC\gamma^{+/+}$  neurons; ### $P < 0.001$  versus corresponding  $cPKC\gamma^{+/+}$  cortical neurons with the same treatment. Scale bar = 100  $\mu$ m.

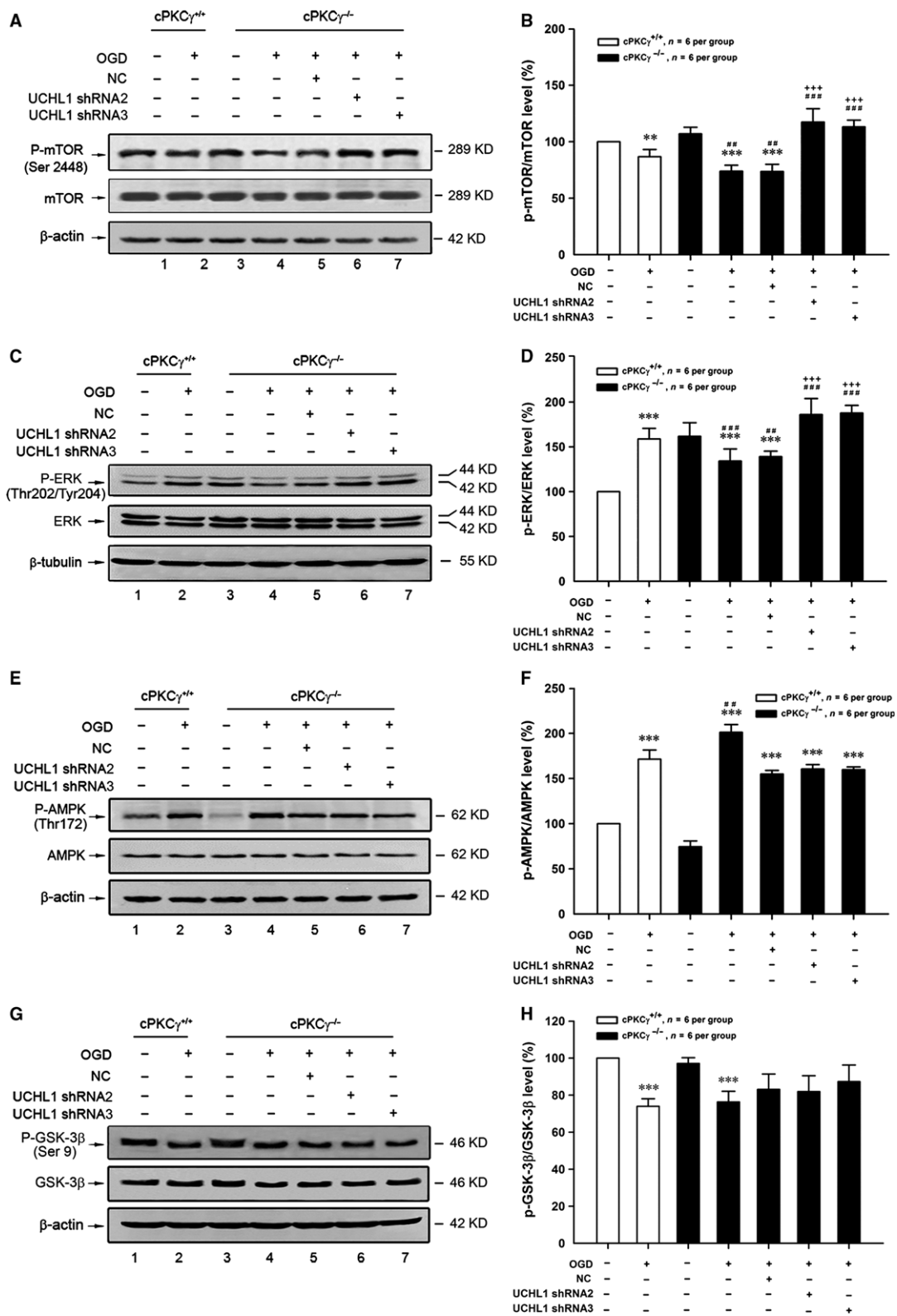


**Fig. 8** Effects of UCHL1 on the expression of mTOR, ERK, AMPK and GSK-3 $\beta$  in cortical neurons after 1-hr OGD/24-hr R. Representative results of (A, C, E and G) and quantitative analysis (B, D, F and H) of Western blot showed the effects of UCHL1 shRNA treatments on the phosphorylation levels of mTOR, ERK, AMPK, GSK-3 $\beta$  from Normoxia and OGD groups of cPKC $\gamma^{+/+}$  and cPKC $\gamma^{-/-}$  cortical neurons ( $n = 6$  per group), respectively. \*\*\* $P < 0.001$ , \*\* $P < 0.01$  versus Normoxia of cPKC $\gamma^{+/+}$  neurons; ### $P < 0.001$ , ## $P < 0.01$  versus corresponding cPKC $\gamma^{+/+}$  cortical neurons with the same treatment; +++ $P < 0.001$  versus NC with the same treatment.

$n = 6$  per group). However, UCHL1 shRNA 2 and 3 treatments could significantly enhance the levels of P-mTOR in cPKC $\gamma^{-/-}$  neurons with OGD treatment (Fig. 8A and B,  $P < 0.001$ ,  $n = 6$  per group).

It is generally known that ERK, AMPK and GSK-3 $\beta$  can regulate the phosphorylation of mTOR [38–40]. We found the phosphorylation of ERK (P-ERK) significantly decreased in the cPKC $\gamma^{-/-}$  neurons compared with cPKC $\gamma^{+/+}$  neurons after 1-hr OGD/24-hr R treatment (Fig. 8C and D,  $P < 0.001$ ,  $n = 6$  per group). UCHL1 shRNA 2 and 3 treatments could significantly enhance the level of P-ERK (Fig. 8C and D,  $P < 0.001$ ,  $n = 6$  per group), which was consistent with the change of P-mTOR.

In addition, the phosphorylation level of AMPK obviously increased after 1-hr OGD/24-hr R and further increased in the cPKC $\gamma^{-/-}$  neurons compared with that of cPKC $\gamma^{+/+}$  neurons (Fig. 8E and F,  $P < 0.01$ ,  $n = 6$  per group), but was not altered by UCHL1 shRNA 2 and 3 treatments (Fig. 8E and F,  $P > 0.05$ ,  $n = 6$  per group). At the same time, the phosphorylation level of GSK-3 $\beta$  obviously decreased after 1-hr OGD/24-hr R (Fig. 8G and H,  $P < 0.001$ ,  $n = 6$  per group), but was altered by neither cPKC $\gamma$  gene knockout nor UCHL1 shRNAs (Fig. 8G and H,  $P > 0.05$ ,  $n = 6$  per group). These results indicate that down-regulation of UCHL1 mediated by cPKC $\gamma$  may decrease OGD-induced autophagy *via* ERK-mTOR pathway.

## Discussion

cPKC $\gamma$  is ubiquitously expressed in the central nervous system [41], which results in much attention in exploring its roles in brain injury. In this study, we found cPKC $\gamma$  knockout could aggravate the neurological deficits which could be proved by neurological score and behavioural tests and increase the infarct volume of mice with ischaemic stroke. Simultaneously, the experiments *in vitro* showed that lack of cPKC $\gamma$  could decrease the survival of OGD-treated primary cortical neurons as well. Our results further validate that endogenous cPKC $\gamma$  protein may be beneficial to neuronal survival and improve stroke outcome.

The localization of UCHL1 is also restricted to neurons. The significant elevation of UCHL1 in CSF and serum is found in the traumatic brain injury (TBI) patients and rats subjected to MCAO, which may be correlated with injury severity and survival outcome of brain injuries [22, 23, 42]. In this study, we observed the same change in CSF and serum of mice with 1-hr MCAO/24-hr R treatment. Because UCHL1 is a neuronal-specific protein, the elevated UCHL1 levels in CSF and serum should be due to its release by neurons. Therefore, we detected the level of UCHL1 in culture medium of primary mouse cortical neurons. The results showed that the level of UCHL1 obviously increased in culture medium following 1-hr OGD/24-hr R. We also observed the protein expression of UCHL1 in neurons. Our results showed that both 1-hr MCAO/24-hr R and 1-hr OGD/24-hr R

treatments could obviously decrease the protein expression of UCHL1. The UCHL1 inhibitor and shRNAs significantly increased the cell survival of cortical neurons with 1-hr OGD/24-hr R treatment, indicating that UCHL1 may aggravate 1-hr OGD/24-hr R-induced cortical neuron injuries. Furthermore, we found that cPKC $\gamma$  knockout did not affect the release of UCHL1 by neurons, while increased the protein expression of UCHL1 in cortical neurons after MCAO or OGD, indicating that down-regulation of UCHL1 mediated by cPKC $\gamma$  may protect neurons against ischaemic injuries. We next tested whether the increase in UCHL1 expression was determined by its protein degradation or mRNA level. We found that the proteasome inhibitor did not alter the UCHL1 protein expression of cPKC $\gamma^{-/-}$  neurons following 1-hr OGD/24-hr R. However, the UCHL1 mRNA expression of cortical neurons significantly decreased after 1-hr OGD/24-hr R and increased in response to cPKC $\gamma$  gene knockout, which was similar to that of the UCHL1 protein expression. Our results indicate that cPKC $\gamma$  may decrease UCHL1 protein expression *via* lowering the mRNA level rather than its protein degradation.

Recently, a functional NF- $\kappa$ B response element is identified in the UCHL1 promoter region, and it has been reported that NF- $\kappa$ B activation suppressed UCHL1 gene transcription [35, 36]. NF- $\kappa$ B complex mainly includes the p65, p50 and NF- $\kappa$ B inhibitor alpha (I $\kappa$ B- $\alpha$ ) subunit [43]. The I $\kappa$ B- $\alpha$  is the most frequent expressed form of NF- $\kappa$ B inhibitors in the nervous system [44]. Various phosphorylation sites (S32, S36 and Y42) within I $\kappa$ B- $\alpha$  have been demonstrated to be important in regulating NF- $\kappa$ B activation [45]. NF- $\kappa$ B is activated through the phosphorylation of I $\kappa$ B- $\alpha$  which promotes to release NF- $\kappa$ B into nuclear and binds to the promoter sites of target genes. Several studies have shown that PKC $\theta$ , PKC $\zeta$ , PKC $\delta$  and aPKC are critical for activation of NF- $\kappa$ B in T cell, monocyte, macrophage, epithelial cell, endothelial cell and microglia, respectively [46–51]. The PKC inhibitor can inhibit the phosphorylation of I $\kappa$ B- $\alpha$  and decelerate the degradation of I $\kappa$ B- $\alpha$  [52]. In this study, we observed that the phosphorylation of I $\kappa$ B- $\alpha$  (Ser 32) significantly increased after OGD but decreased in response to cPKC $\gamma$  gene knockout. Our results suggest that cPKC $\gamma$  may down-regulate UCHL1 mRNA expression through the I $\kappa$ B- $\alpha$ /NF- $\kappa$ B pathway.

It is generally known that oxidative stress and apoptosis are involved in brain damage after cerebral ischaemia [25, 53]. In this study, we found that cPKC $\gamma$  gene knockout significantly enhanced OGD-induced oxidative stress (data not shown) and apoptosis, indicating that cPKC $\gamma$  may exert neuroprotective effects against oxidative stress and apoptosis during ischaemic injury. UCHL1 is found to increase cellular ROS level by up-regulating H<sub>2</sub>O<sub>2</sub> generation in melanoma cells and induce apoptosis in spermatocyte of mice with cryptorchidism and breast tumour cells [54–56]. Then, we explored whether cPKC $\gamma$  could regulate oxidative stress and apoptosis through UCHL1 in the present study. We found that UCHL1 inhibitor or various shRNAs failed to affect oxidative stress and apoptosis induced by



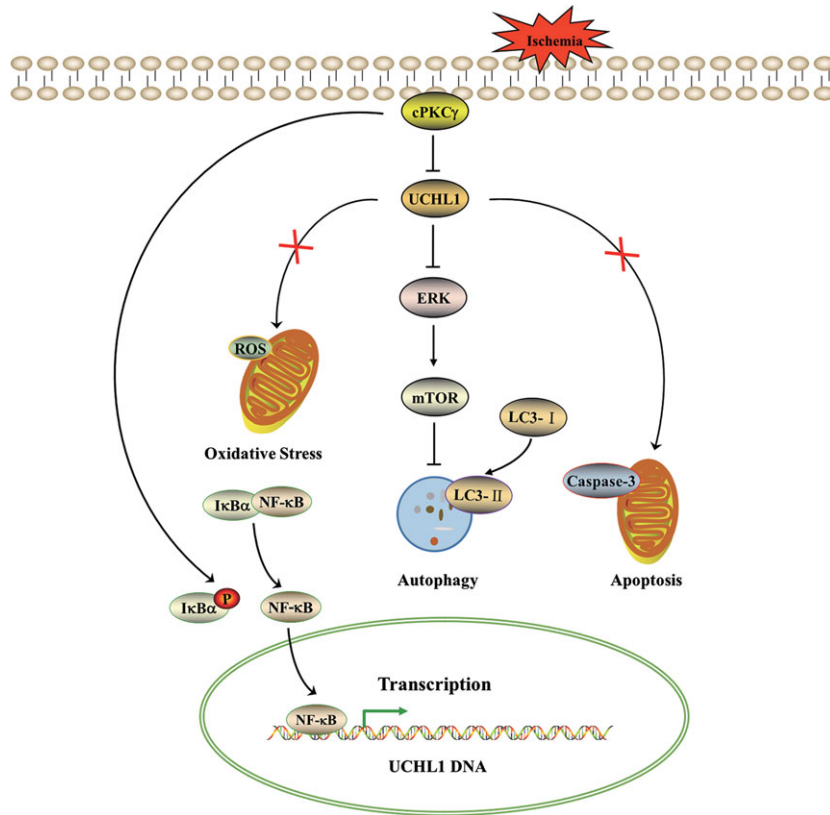


**Fig. 9** Schematic diagram of the effect of cPKC $\gamma$ -UCHL1 on autophagy through ERK-mTOR pathway in cerebral ischaemic injuries. cPKC $\gamma$  reduces UCHL1 protein expression *via* decreasing its mRNA level regulated by the I $\kappa$ B- $\alpha$ /NF- $\kappa$ B pathway in cortical neurons following ischaemic neuronal injuries. UCHL1 positively regulates autophagy through ERK-mTOR pathway, which may aggravate cerebral ischaemic injuries, instead of oxidative stress and apoptosis.

OGD treatment in cPKC $\gamma^{-/-}$  neurons. Our results suggest that UCHL1 may not be involved in the effects of cPKC $\gamma$  on oxidative stress and apoptosis during ischaemic injury.

In recent years, more attention has been paid to the role of autophagy in ischaemic injuries. However, the role of autophagy in ischaemic stroke is still controversial. Induction of autophagy by nicotinamide phosphoribosyltransferase increases the cell survival rate and simultaneously decreases the LDH leakage of primary neurons with 2-hr OGD treatment [57]. But other studies have reported that activation of autophagy can aggravate cortical neural cell injury following 1-hr focal cerebral ischaemia/24-hr R [58, 59]. Our results showed that the ratio of LC3-II/total LC3, related with the level of autophagosome formation, evidently increased after 1-hr MCAO/24-hr R or 1-hr OGD/24-hr R treatment. BafA1, an autophagy inhibitor, could increase the cell survival rate and simultaneously decrease the cell death rate of cortical neurons with 1-hr OGD/24-hr R treatment, suggesting autophagy may be involved in a neuronal death pathway following ischaemic neuronal injury. In addition, we found that cPKC $\gamma$  knockout could significantly increase the conversion of LC3-I to LC3-II in peri-infarct region of mice with ischaemic stroke and primary cultured cortical neurons with OGD treatment, suggesting cPKC $\gamma$  can negatively regulate autophagy induced by ischaemic neuronal injury. Inhibition of UCHL1 activity by LDN treatment is reported to regulate activation of the autophagy pathway in  $\alpha$ -syn tg mice and  $\alpha$ -syn over expressing cells [60]. Then, we explored whether cPKC $\gamma$  could regulate autophagy through UCHL1. We observed

that both LDN and UCHL1 shRNA treatments significantly decreased the ratio of LC3-II/total LC3-I in cPKC $\gamma^{-/-}$  neurons, suggesting that UCHL1 is involved in the effect of cPKC $\gamma$  on autophagy following ischaemic neuronal injury.

Autophagy is a bulk protein degradation system that is involved in multiple cellular processes. The kinase mTOR is a considerable regulator of autophagy induction, when regulating mTOR positively can suppress autophagy and inhibiting mTOR can promote it. Rapamycin which directly inhibits mTOR is the most commonly used and specific inducer of autophagy [61]. Our results showed that the mTOR phosphorylation level obviously decreased after 1-hr OGD/24-hr R, what's more, cPKC $\gamma$  knockout resulted in more reduction in P-mTOR. However, UCHL1 shRNAs could significantly enhance the mTOR phosphorylation in the cPKC $\gamma^{-/-}$  neurons with OGD treatment. ERK, one of the upstream targets of mTOR, can positively regulate mTOR activation and inhibit autophagy flux [62]. The mTOR can be inhibited by AMPK which regulates intracellular energy status by sensing the AMP/ATP ratio [63]. GSK-3 $\beta$  is also generally known to be a negative regulator of mTOR, when inactivating GSK-3 $\beta$  by phosphorylation leads to the activation of mTOR signalling pathways [64]. The inhibition of PKC by GF-109203X can activate GSK-3, providing evidence that the activity of GSK-3 is negatively regulated by PKC [24]. Our results showed that consistent with the trend of P-mTOR, cPKC $\gamma$  knockout significantly decreased the ERK phosphorylation following 1-hr OGD/24-hr R,



while UCHL1 shRNAs obviously enhanced the level of P-ERK. The phosphorylation of AMPK significantly increased after 1-hr OGD/24-hr R, further increased in the cPKC $\gamma^{-/-}$  neurons, but was not altered by various UCHL1 shRNA treatments. The phosphorylation of GSK-3 $\beta$  obviously reduced after 1-hr OGD/24-hr R, but was neither altered by cPKC $\gamma$  knockout nor UCHL1 shRNAs. These results above suggest that cPKC $\gamma$ /UCHL1 may regulate autophagy through ERK-mTOR pathway during ischaemic neuronal injury.

## Conclusion

In summary, our results indicate that down-regulation of UCHL1 mediated by cPKC $\gamma$  may negatively regulate autophagy through ERK-mTOR pathway, which alleviates ischaemic neuronal injury (Fig. 9). However, further studies about the mechanism how UCHL1 can regulate ERK-mTOR pathway will be required.

## References

- Liu M, Wu B, Wang WZ, *et al.* Stroke in China: epidemiology, prevention, and management strategies. *Lancet Neurol.* 2007; 6: 456–64.
- Writing Group M, Mozaffarian D, Benjamin EJ, *et al.* Heart disease and stroke statistics-2016 update: a report from the American heart association. *Circulation.* 2016; 133: e38–360.
- Krupinski J, Stevin MA, Kumar P, *et al.* Protein kinase C expression and activity in the human brain after ischaemic stroke. *Acta Neurol Exp (Wars).* 1998; 58: 13–21.
- Matsumoto S, Shamloo M, Matsumoto E, *et al.* Protein kinase C-gamma and calcium/calmodulin-dependent protein kinase II-alpha are persistently translocated to cell membranes of the rat brain during and after middle cerebral artery occlusion. *J Cereb Blood Flow Metab.* 2004; 24: 54–61.
- Liu Y, Li J, Yang J, *et al.* Inhibition of PKCgamma membrane translocation mediated morphine preconditioning-induced neuroprotection against oxygen-glucose deprivation in the hippocampus slices of mice. *Neurosci Lett.* 2008; 444: 87–91.
- Hamabe W, Fujita R, Ueda H. Insulin receptor-protein kinase C-gamma signaling mediates inhibition of hypoxia-induced necrosis of cortical neurons. *J Pharmacol Exp Ther.* 2005; 313: 1027–34.
- Hayashi S, Ueyama T, Kajimoto T, *et al.* Involvement of gamma protein kinase C in estrogen-induced neuroprotection against focal brain ischemia through G protein-coupled estrogen receptor. *J Neurochem.* 2005; 93: 883–91.
- Li J, Niu C, Han S, *et al.* Identification of protein kinase C isoforms involved in cerebral hypoxic preconditioning of mice. *Brain Res.* 2005; 1060: 62–72.
- Niu C, Li J, Cui X, *et al.* Changes in cPKC isoform-specific membrane translocation and protein expression in the brain of hypoxic preconditioned mice. *Neurosci Lett.* 2005; 384: 1–6.
- Bu X, Zhang N, Yang X, *et al.* Proteomic analysis of cPKCbetall-interacting proteins involved in HPC-induced neuroprotection against cerebral ischemia of mice. *J Neurochem.* 2011; 117: 346–56.
- Matsumoto S, Murozono M, Nagaoka D, *et al.* Isoflurane inhibits protein kinase Cgamma and calcium/calmodulin dependent protein kinase ii-alpha translocation to synaptic membranes in ischemic mice brains. *Neurochem Res.* 2008; 33: 2302–9.
- Zhang N, Yin Y, Han S, *et al.* Hypoxic preconditioning induced neuroprotection against cerebral ischemic injuries and its cPKCgamma-mediated molecular mechanism. *Neurochem Int.* 2011; 58: 684–92.
- Wilson PO, Barber PC, Hamid QA, *et al.* The immunolocalization of protein gene product 9.5 using rabbit polyclonal and mouse monoclonal antibodies. *Br J Exp Pathol.* 1988; 69: 91–104.
- Wilkinson KD, Lee KM, Deshpande S, *et al.* The neuron-specific protein PGP 9.5 is a ubiquitin carboxyl-terminal hydrolase. *Science.* 1989; 246: 670–3.
- Liu Y, Fallon L, Lashuel HA, *et al.* The UCH-L1 gene encodes two opposing enzymatic activities that affect alpha-synuclein degradation and Parkinson's disease susceptibility. *Cell.* 2002; 111: 209–18.
- Osaka H, Wang YL, Takada K, *et al.* Ubiquitin carboxy-terminal hydrolase L1 binds to and stabilizes monoubiquitin in neuron. *Hum Mol Genet.* 2003; 12: 1945–58.
- Setuie R, Wada K. The functions of UCH-L1 and its relation to neurodegenerative diseases. *Neurochem Int.* 2007; 51: 105–11.
- Carriero C, Forrest AR, Santoro C, *et al.* Expression analysis of the long non-coding RNA antisense to Uchl1 (AS Uchl1) during dopaminergic cells' differentiation *in vitro* and in neurochemical models of Parkinson's disease. *Front Cell Neurosci.* 2015; 9: 114. doi: 10.3389/fncel.2015.00114
- Tramutola A, Di Domenico F, Barone E, *et al.* It is all about (U)biqutin: role of altered ubiquitin-proteasome system and UCHL1 in Alzheimer disease. *Oxid Med Cell Longev.* 2016; 2016: 2756068 doi: 10.1155/2016/2756068.
- Xu EH, Tang Y, Li D, *et al.* Polymorphism of HD and UCHL-1 genes in Huntington's disease. *J Clin Neurosci.* 2009; 16: 1473–7.
- Johnston SC, Riddle SM, Cohen RE, *et al.* Structural basis for the specificity of ubiquitin C-terminal hydrolases. *EMBO J.* 1999; 18: 3877–87.
- Liu MC, Akinyi L, Scharf D, *et al.* Ubiquitin C-terminal hydrolase-L1 as a biomarker for ischemic and traumatic brain injury in rats. *Eur J Neurosci.* 2010; 31: 722–32.
- Ren C, Zoltewicz S, Guingab-Cagmat J, *et al.* Different expression of ubiquitin C-terminal hydrolase-L1 and alphaspectrin

## Acknowledgements

The author(s) disclosed receipt of the following financial support for the research, authorship and/or publication of this article: National Natural Science Foundation of China (Grant No. 81400948, 31471142 and 31671205), Beijing Natural Science Foundation (Grant No. 7141001) and Scientific Research Common Program of Beijing Municipal Commission of Education (KM201410025004).

LZ and JL conceived and designed research; DZ, SW and SH performed experiments; DZ, SW and YL analysed data; LZ, DZ and SH interpreted results of experiments; DZ, SW and YL prepared figures; LZ, DZ and SW drafted manuscript; LZ and JL edited and revised manuscript; JL approved final version of manuscript.

## Conflict of interest

The authors confirm that there are no conflict of interests.

- in ischemic and hemorrhagic stroke: potential biomarkers in diagnosis. *Brain Res.* 2013; 1540: 84–91.
24. **Zhao L, Chu CB, Li JF, et al.** Glycogen synthase kinase-3 reduces acetylcholine level in striatum via disturbing cellular distribution of choline acetyltransferase in cholinergic interneurons in rats. *Neuroscience.* 2013; 255: 203–11.
  25. **Wang G, Weng YC, Han X, et al.** Lipocalin-2 released in response to cerebral ischaemia mediates reperfusion injury in mice. *J Cell Mol Med.* 2015; 19: 1637–45.
  26. **Rodriguez R, Santiago-Mejia J, Gomez C, et al.** A simplified procedure for the quantitative measurement of neurological deficits after forebrain ischemia in mice. *J Neurosci Methods.* 2005; 147: 22–8.
  27. **Balkaya M, Krober J, Gertz K, et al.** Characterization of long-term functional outcome in a murine model of mild brain ischemia. *J Neurosci Methods.* 2013; 213: 179–87.
  28. **Chen J, Zhang C, Jiang H, et al.** Atorvastatin induction of VEGF and BDNF promotes brain plasticity after stroke in mice. *J Cereb Blood Flow Metab.* 2005; 25: 281–90.
  29. **Tennant KA, Jones TA.** Sensorimotor behavioral effects of endothelin-1 induced small cortical infarcts in C57BL/6 mice. *J Neurosci Methods.* 2009; 181: 18–26.
  30. **Lubjuhn J, Gastens A, von Wilpert G, et al.** Functional testing in a mouse stroke model induced by occlusion of the distal middle cerebral artery. *J Neurosci Methods.* 2009; 184: 95–103.
  31. **Wexler EJ, Peters EE, Gonzales A, et al.** An objective procedure for ischemic area evaluation of the stroke intraluminal thread model in the mouse and rat. *J Neurosci Methods.* 2002; 113: 51–8.
  32. **Wei H, Li Y, Han S, et al.** cPKCgamma-Modulated Autophagy in Neurons Alleviates Ischemic Injury in Brain of Mice with Ischemic Stroke Through Akt-mTOR Pathway. *Transl Stroke Res.* 2016; 7: 497–511.
  33. **Spalenza V, Girolami F, Bevilacqua C, et al.** Identification of internal control genes for quantitative expression analysis by real-time PCR in bovine peripheral lymphocytes. *Vet J.* 2011; 189: 278–83.
  34. **Livak KJ, Schmittgen TD.** Analysis of relative gene expression data using real-time quantitative PCR and the 2(-Delta Delta C(T)) Method. *Methods.* 2001; 25: 402–8.
  35. **Wang R, Zhang M, Zhou W, et al.** NF-kappaB signaling inhibits ubiquitin carboxyl-terminal hydrolase L1 gene expression. *J Neurochem.* 2011; 116: 1160–70.
  36. **Guglielmotto M, Monteleone D, Boido M, et al.** Abeta1-42-mediated down-regulation of Uch-L1 is dependent on NF-kappaB activation and impaired BACE1 lysosomal degradation. *Aging Cell.* 2012; 11: 834–44.
  37. **Huang XP, Ding H, Lu JD, et al.** Autophagy in cerebral ischemia and the effects of traditional Chinese medicine. *J Integr Med.* 2015; 13: 289–96.
  38. **Wang Y, Li Y, Di C, et al.** Protective effects of transient receptor potential canonical channels on oxygen-glucose deprivation-induced cell injury in neurons and PC12 cells. *NeuroReport.* 2016; 27: 1072–80.
  39. **Gong X, Wang H, Ye Y, et al.** miR-124 regulates cell apoptosis and autophagy in dopaminergic neurons and protects them by regulating AMPK/mTOR pathway in Parkinson's disease. *Am J Transl Res.* 2016; 8: 2127–37.
  40. **Liu RJ, Fuchikami M, Dwyer JM, et al.** GSK-3 inhibition potentiates the synaptogenic and antidepressant-like effects of sub-threshold doses of ketamine. *Neuropsychopharmacology.* 2013; 38: 2268–77.
  41. **Saito N, Shirai Y.** Protein kinase C gamma (PKC gamma): function of neuron specific isotype. *J Biochem.* 2002; 132: 683–7.
  42. **Mondello S, Linnet A, Buki A, et al.** Clinical utility of serum levels of ubiquitin C-terminal hydrolase as a biomarker for severe traumatic brain injury. *Neurosurgery.* 2012; 70: 666–75.
  43. **Wan F, Lenardo MJ.** The nuclear signaling of NF-kappaB: current knowledge, new insights, and future perspectives. *Cell Res.* 2010; 20: 24–33.
  44. **Mincheva-Tasheva S, Soler RM.** NF-kappaB signaling pathways: role in nervous system physiology and pathology. *Neuroscientist.* 2013; 19: 175–94.
  45. **Gutierrez H, Davies AM.** Regulation of neural process growth, elaboration and structural plasticity by NF-kappaB. *Trends Neurosci.* 2011; 34: 316–25.
  46. **Coudronniere N, Villalba M, Englund N, et al.** NF-kappa B activation induced by T cell receptor/CD28 costimulation is mediated by protein kinase C-theta. *Proc Natl Acad Sci USA.* 2000; 97: 3394–9.
  47. **Huang X, Chen LY, Doerner AM, et al.** An atypical protein kinase C (PKC zeta) plays a critical role in lipopolysaccharide-activated NF-kappa B in human peripheral blood monocytes and macrophages. *J Immunol.* 2009; 182: 5810–5.
  48. **Wullaert A, Bonnet MC, Pasparakis M.** NF-kappaB in the regulation of epithelial homeostasis and inflammation. *Cell Res.* 2011; 21: 146–58.
  49. **Aveleira CA, Lin CM, Abcouwer SF, et al.** TNF-alpha signals through PKCzeta/NF-kappaB to alter the tight junction complex and increase retinal endothelial cell permeability. *Diabetes.* 2010; 59: 2872–82.
  50. **Gordon R, Singh N, Lawana V, et al.** Protein kinase Cdelta upregulation in microglia drives neuroinflammatory responses and dopaminergic neurodegeneration in experimental models of Parkinson's disease. *Neurobiol Dis.* 2016; 93: 96–114.
  51. **Avila A, Silverman N, Diaz-Meco MT, et al.** The Drosophila atypical protein kinase C-ref (2)p complex constitutes a conserved module for signaling in the toll pathway. *Mol Cell Biol.* 2002; 22: 8787–95.
  52. **Wang Y, Ding M, Chaudhari S, et al.** Nuclear factor kappaB mediates suppression of canonical transient receptor potential 6 expression by reactive oxygen species and protein kinase C in kidney cells. *J Biol Chem.* 2013; 288: 12852–65.
  53. **Chen H, Yoshioka H, Kim GS, et al.** Oxidative stress in ischemic brain damage: mechanisms of cell death and potential molecular targets for neuroprotection. *Antioxid Redox Signal.* 2011; 14: 1505–17.
  54. **Du P, Yao YW, Shi Y, et al.** Uchl1 and its associated proteins were involved in spermatocyte apoptosis in mouse experimental cryptorchidism. *Sheng Li Xue Bao.* 2014; 66: 528–36.
  55. **Xiang T, Li L, Yin X, et al.** The ubiquitin peptidase UCHL1 induces G0/G1 cell cycle arrest and apoptosis through stabilizing p53 and is frequently silenced in breast cancer. *PLoS One.* 2012; 7: e29783.
  56. **Kim HJ, Magesh V, Lee JJ, et al.** Ubiquitin C-terminal hydrolase-L1 increases cancer cell invasion by modulating hydrogen peroxide generated via NADPH oxidase 4. *Oncotarget.* 2015; 6: 16287–303.
  57. **Wang P, Guan YF, Du H, et al.** Induction of autophagy contributes to the neuroprotection of nicotinamide phosphoribosyltransferase in cerebral ischemia. *Autophagy.* 2012; 8: 77–87.
  58. **Zhao Y, Huang G, Chen S, et al.** Folic acid deficiency increases brain cell injury via autophagy enhancement after focal cerebral ischemia. *J Nutr Biochem.* 2016; 38: 41–9.
  59. **Zhao Y, Huang G, Chen S, et al.** Homocysteine Aggravates Cortical Neural Cell Injury through Neuronal Autophagy Over-activation following Rat Cerebral

- Ischemia-Reperfusion. *Int J Mol Sci.* 2016; 17: 1196 doi:10.3390/ijms17081196.
60. **Cartier AE, Ubhi K, Spencer B, et al.** Differential effects of UCHL1 modulation on alpha-synuclein in PD-like models of alpha-synucleinopathy. *PLoS One.* 2012; 7: e34713.
61. **Klionsky DJ, Abeliovich H, Agostinis P, et al.** Guidelines for the use and interpretation of assays for monitoring autophagy in higher eukaryotes. *Autophagy.* 2008; 4: 151–75.
62. **Goncharova EA.** mTOR and vascular remodeling in lung diseases: current challenges and therapeutic prospects. *FASEB J.* 2013; 27: 1796–807.
63. **Zhang L, Wei J, Ren L, et al.** Endosulfan induces autophagy and endothelial dysfunction via the AMPK/mTOR signaling pathway triggered by oxidative stress. *Environ Pollut.* 2017; 220: 843–52.
64. **Hassanian SM, Ardeshiryajimi A, Dinarvand P, et al.** Inorganic polyphosphate promotes cyclin D1 synthesis through activation of mTOR/Wnt/beta-catenin signaling in endothelial cells. *J Thromb Haemost.* 2016; 14: 2261–73.